Thin Solid Films 518 (2009) 1289–1293

Contents lists available at ScienceDirect

Thin Solid Films

journal homepage: www.elsevier.com/locate/tsf

Optical modeling of free electron behavior in highly doped ZnO films

F. Ruske [a,*], A. Pflug [b], V. Sittinger [b], B. Szyszka [b], D. Greiner [c], B. Rech [a]

[a] Helmholtz-Zentrum Berlin für Materialien und Energie, Silicon Photovoltaics, Kekuléstraße 5, 12489 Berlin, Germany
[b] Fraunhofer-Institute for Surface Engineering and Thin Films (IST), Bienroder Weg 54e, 38108 Braunschweig, Germany
[c] Helmholtz-Zentrum Berlin für Materialien und Energie, Heterogeneous Material Systems, Glienicker Straße 100, 14109 Berlin, Germany

ARTICLE INFO

Available online 8 May 2009

Keywords:
Transparent conductive oxide
Zinc oxide
Optical properties
Electrical properties
Charge carrier scattering
Effective mass
Optical characterization

ABSTRACT

Transparent conductive oxides (TCOs) with tailor-made electrical and optical properties are essential for a variety of applications. The linkage of optical and electrical properties in these films is usually described by the Drude theory despite the fact, that earlier investigations have already shown that the Drude theory fails to accurately describe optical properties. In this work we use an extension to the Drude theory to model optical spectra of reactively sputtered ZnO:Al thin films. The model uses a simple analytic expression, which can describe the general course of the dielectric function as calculated by others with more elaborate models. Using this approach optical spectra can be accurately modeled with low computational effort and reliable values for plasma frequency and damping can be obtained. By comparing these results with Hall measurements we derived the effective mass of free carriers m^* in the conduction band as a function of carrier concentration. The results clearly showed the non-parabolicity of the conduction band for high doping levels. Using the band structure proposed by Pisarkiewicz and assuming an effective mass of 0.24 electron masses at the conduction band minimum we derived a non-parabolicity parameter of ~0.27 (2) eV^{-1}. Finally we used the values for the effective mass to determine carrier mobility from optical measurements. Contradictions to Hall measurements can be explained by the effect of grain boundary scattering.

1. Demands on modern TCO materials

The application fields of transparent conductive oxides (TCOs) are vast and increasing in the last years. Besides the flat panel industry, photovoltaics has emerged as a major industrial branch in need for high quality transparent conducting oxides [1,2]. The development of large area deposition processes for these layers has experienced a boost with industrialization of thin-film concepts, e.g. solar cells based on thin-film silicon or compound semiconductors like CuInS and related materials.

A simple requirement posed on the TCO film in this context is a high optical transmission for photon energies above the bandgap of the absorber material used. As an example the bandgaps of polycrystalline and hydrogenated microcrystalline silicon are around 1.1 eV. This means that the spectral range in which the TCO layer should exhibit high transmission will reach up to 1100 nm. This requirement is not met by many TCO films as, depending on doping level, they can have a considerable absorption in this range.

The decreased transmission towards higher wavelengths is caused by free carrier absorption. This means that the optical behavior of TCO films is strongly linked to the electrical transport properties. This is described by the Drude theory, which is presented in Section 2. In this paper we will discuss the adequacy of the Drude model for modeling of optical spectra. As a consequence a simple analytic expression, that yields more accurate results and still allows an evaluation with low computational effort, will be used as an extension to the Drude theory.

The results of the modeling procedure are used to investigate the linkage of optical and electrical performance of the films used in this work. As will be seen the effective mass m^* of the electrons in the conduction band is a key parameter to understand the link of optical and electrical behavior of TCO materials. Only the assumption of a non-parabolic conduction band in ZnO leads to an accurate determination of carrier concentration from optical spectroscopy.

Finally, the information gained on the conduction band form is used to also determine the carrier mobility from the optical spectra. The large amount of samples included in this study provides the basis for a detailed investigation of the carrier concentration range, in which the carriers undergo similar scattering processes in DC transport and upon optical excitation.

2. Drude theory and extensions

The trade-off between optical transmission and electrical conductivity of TCO layers demands a profound knowledge of the connection of the two material properties. The basic theory of the optical behavior of free carriers in solids has been formulated by Drude and is described in various textbooks and articles [3]. In his

* Corresponding author. Tel.: +49 30 8062 1375; fax: +49 30 8062 1333.
E-mail address: florian.ruske@helmholtz-berlin.de (F. Ruske).

0040-6090/$ – see front matter © 2009 Elsevier B.V. All rights reserved.
doi:10.1016/j.tsf.2009.03.218

theory the susceptibility accounting for the free carriers can be expressed as

$$\chi^{\mathrm{FE}} = -\frac{\omega_{\mathrm{p}}^2}{\omega^2 + i\omega\omega_\tau} \tag{1}$$

In this expression ω_{p} denotes the plasma frequency and ω_τ is a damping term. ω_{p} is a function of the carrier density N_{e}, while the damping depends on the mobility μ:

$$\omega_{\mathrm{p}}^2 = \frac{e^2 N_{\mathrm{e}}}{\varepsilon_0 m^*_{\mathrm{opt}}} \tag{2}$$

$$\omega_\tau = \frac{e}{m^*_{\mathrm{opt}}\mu} \tag{3}$$

In the two expressions m^*_{opt} denotes the electron effective mass [4].

Due to this effect a TCO film, that is transparent in the visible spectral range, will reflect light in the long wavelength region, with the plasma frequency roughly defining the border between the two regimes. The damping defines the steepness of the transition. As the plasma frequency shifts to higher frequencies with increasing carrier concentration, the demand for high transmission at a specific wavelength will set an upper limit for the carrier concentration, while optical transmission below the plasma frequency and conductivity will both benefit from high mobilities.

The Drude expression has been used by various authors to derive information on free carrier behavior in ZnO thin films by evaluation of reflection data [6,7], transmission spectra [8] or ellipsometric spectra [9,10]. However, deviations from the Drude theory can be observed if both transmission and reflection data are taken into account. The main reason is a frequency dependance of the damping frequency in highly doped TCOs for frequencies above the plasma frequency. Generally this is expressed in a frequency-dependant real part of the dynamic resistivity ρ. It follows a power law $\rho \infty \omega^\alpha$, in which α indicates the dominant scattering behavior [11].

The theory was applied to ITO films by Hamberg et al. [12] and showed an accurate description of the dielectric function. The theory was later also applied to ZnO thin films [13].

Unfortunately the solution of the underlying equations are challenging in terms of computation and hence difficult to implement for fitting of optical spectra. Thus other authors implemented analytic functions in order to describe the frequency dependant damping [14]. We used a simplified expression already describes in [15]. In this approach an analytic expression is used to describe the frequency dependance of the damping and $\omega_\tau(\omega)$ is expressed as

$$\omega_\tau(\omega) = f(\omega)\omega_{\tau 0} + (1 - f(\omega))\omega_{\tau 1}\left(\frac{\omega}{\omega_{\mathrm{tr}}}\right)^\alpha \tag{4}$$

$$\text{where} \quad f(\omega) = \frac{1}{1 + \exp\frac{\omega - \omega_{\mathrm{tr}}}{\sigma}} \tag{5}$$

In this case the parameter $\omega_{\tau 0}$, describing the low frequency limit of the damping frequency, has to be used for calculation of carrier mobility using Eq. (3). It is reasonable to set the exponent $\alpha = -\frac{3}{2}$, which is characteristic for ionized impurity scattering [11,16].

This extended Drude approach has been used to evaluate optical transmission and reflection data in the visible and the near-infrared spectral range. The effective mass m^*_{opt} of the free carriers is derived by correlating values for plasma frequency obtained from fitting with carrier concentration determined with Hall measurements. Values obtained in this work are compared to results from literature. The amount of samples and data available enables the estimation of the form of the conduction band and the comparison to models for its non-parabolicity.

3. Experimental details

The samples used for this study were prepared in a vertical in-line sputtering coater by reactive magnetron sputtering. A dual magnetron setup driven by a 40 kHz discharge was employed. The working point was controlled by a closed loop control, adjusting target power in order to stabilize the desired oxygen partial pressure inside the chamber. Details on the setup and process control can be found in [17,18].

In order to achieve films with varying free electron densities, metallic targets with Al concentrations ranging from 0.3 to 2 weight percent (wt.%) were used. Despite this variation, the control of electron density is difficult, as the Al concentration of the films depends on deposition conditions [19] and the doping efficiency strongly varies between different films. This lead to films with a wide range of different carrier concentrations, ranging from 2 to $9 \cdot 10^{20}$ cm^{-3}.

A double beam spectrophotometer (Varian Cary-5) was used to measure optical transmission and reflection in the spectral range from 250 to 2500 nm. Additionally spectroscopic ellipsometry at variable angle, using a Sentech SE 850, was carried out from 350 to 850 nm. Although the spectroscopic ellipsometry provides almost no information on the free electrons in the ZnO films due to the limited spectral range, it can be used to accurately determine film thickness, surface roughness and the dielectric function in the visible range. In practice, ellipsometric and photometric spectra are evaluated simultaneously by a software developed by Fraunhofer IST as already described in [15]. The software offers the possibility to vary the analytic expressions used to describe the dielectric function of the investigated materials. From the proposed dielectric functions theoretical spectra are computed and compared to the measured ones. The deviation between the curves is calculated as a weighted square and minimized using the Marquardt–Levenberg algorithm. This allows the estimation of an absolute error of the fitting parameters and correlations among them.

For the ZnO:Al films a dielectric function of the form of Eq. (6) was used [13]

$$\overline{\varepsilon}(\omega) = \varepsilon_\infty + \chi^{\mathrm{BG}} + \chi^{\mathrm{FE}}. \tag{6}$$

In this expression χ^{BG} denotes the contribution of the band gap absorption, which was modeled using the oscillator proposed by Leng [20], while ε_∞ describes the contribution of resonances at higher frequencies. The model is adequate, as resonances like phonons lie well outside the studied spectral range.

In order to describe the surface roughness of the ZnO-layers an additional effective medium layer was used. Its dielectric function was calculated as mixture of ZnO:Al and air ($\overline{\varepsilon} = 1$) using Bruggeman's theory [21], with a fixed volume concentration of 50% each.

In addition to optical spectroscopy, Hall measurements were conducted on all samples in order to determine carrier concentration and mobility. All measurements were carried out in van der Pauw geometry at room temperature. Measurements were repeated using different measuring currents. From this repetition and contact permutation in the van der Pauw scheme [22] the error of the measurement can be calculated.

4. Results

4.1. Modeling of measured data

In order to show the problems associated with the simple Drude model some spectra have been evaluated using both the simple Drude model and the extended expression including a frequency dependant damping. Fig. 1 shows optical transmission and reflection for two different films and the modeled spectra obtained using both

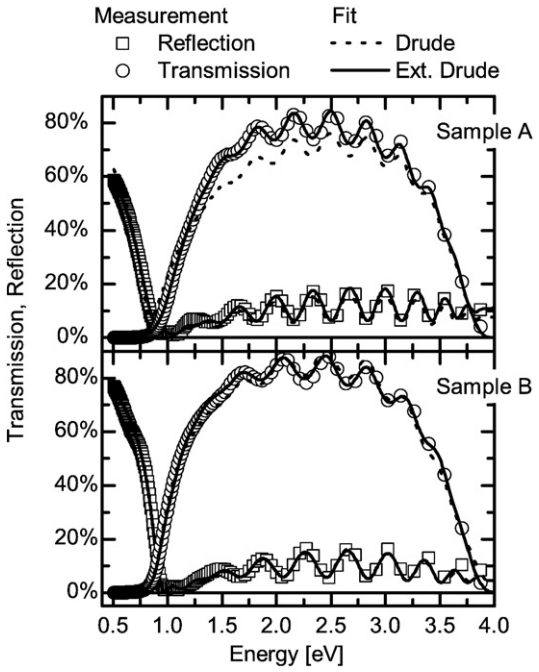

Fig. 1. Measured optical transmission and reflection of two different ZnO:Al films and spectra fitted to them. The dotted line indicates the spectrum calculated using the Drude theory, the solid line was calculated using the extended Drude theory with frequency dependant damping. The simple Drude theory can describe various spectra, but fails for others. Usually the transmission below the plasma edge is underestimated. Film properties and fit results can be found in Table 1.

expressions for free electron behavior. Sample A has been deposited at a substrate temperature of 200 °C, using a target with an aluminium concentration of 2weight percent (wt.%), whereas sample B was deposited at 260 °C with a target containing 0.5 wt.% aluminium.

Not shown are the ellipsometric spectra that have been modeled simultaneously. Examples can be found in [15]. Their inclusion greatly reduces the errors on film thickness and the refractive index in the visible range. Only onsets of free electron absorption is contained in these spectra due to the limited spectral range of the ellipsometer used.

The modeling of free electron behavior gains importance in the near infrared part of the spectrum for photon energies below 2 eV. As becomes apparent for sample A, the evaluation using the Drude theory and the extended theory can lead to substantial differences. The Drude theory fails to describe the measured transmission and reflection curves simultaneously and the absorption below the plasma edge is overestimated.

It should be mentioned that the reflection curve is described well by the Drude theory as the frequency dependance of the damping only plays a role for photon energies above the plasma energy. This is the main reason for a successful application of the Drude theory to describe optical reflection spectra as in [6] and [7].

The parameters obtained by modeling of the spectra shown in Fig. 1 are listed in Table 1. As can be seen the film thicknesses between both models only show slight differences below 1% which is mostly due to the use of ellipsometric data. The values perfectly correspond to values measured by a mechanical stylus instrument.

For plasma frequency and damping the fitting algorithm yields a numerical error around 0.1% and no correlation to other fitting parameters, apart from a weak correlation between plasma frequency and film thickness. Despite this low numerical error we assume the real error to be around 2% for both plasma frequency and damping.

The poor performance of the Drude theory for sample A as seen in Fig. 1 is also reflected in a higher mean squared error (MSE) between measurement and modeled curve, while the value is almost identical for the two models in the case of sample B. As a result significantly

Table 1
Fitting parameters obtained from the fits shown in Fig. 1 for both samples.

		Sample A		Sample B	
		Drude	Ext. drude	Drude	Ext. drude
d_{layer}	[nm]	786.7	783.1	669.9	675.2
d_{top}	[nm]	26.3	19.8	33.1	32.7
ω_p	[10^3/cm]	12.39	13.00	13.40	13.43
$\omega_\tau/\omega_{\tau 0}$	[10^3/cm]	143	1.89	0.83	0.85
MSE		0.028	0.019	0.020	0.018

For the calculation of carrier concentration and mobility via Eqs. (2) and (3) an effective mass of 0.4 times the electron mass has been assumed. MSE denotes the mean squared error of the modeled spectrum in respect to the measurement.

different values are obtained for plasma frequency and damping, which differ for both models in the case of sample A but are almost equal for sample B.

The result is alarming if we consider that the simple Drude model describes the reflection data quite well. Thus it could be assumed that the Drude theory allows for a good description of measured data if only the reflection spectrum is studied. Instead our result shows that the derived plasma frequency can be inaccurate, in the case of sample A the deviation is around 5%.

In order to achieve more reliable values for the optical constants n and k we highly recommend to use two measured quantities for an analysis of the dielectric function of a film. This can be transmission and reflection data, as in this study, or ellipsometric data where Ψ and Δ can be obtained from a single measurement as in [9] or [10]. In addition an appropriate model has to be chosen for free electron susceptibility.

4.2. Determination of conductivity effective mass as a function of carrier concentration

With the results of the previous section in mind we chose to use the frequency dependant damping term for evaluation of all of the samples included in this study. From the modeling we obtained ω_p and ω_τ for a large number of samples. All samples also underwent investigation by Hall measurement at room temperature, from which N_e^{Hall} and μ^{Hall} were derived. From Eq. (2) we expect a linear dependance of N_e on ω_p^2. The relation is checked in Fig. 2, where we plot the carrier concentration determined by Hall measurements as a function of the square of the plasma frequency. The additional lines indicate the expected behavior for different fixed values for the effective mass m^*.

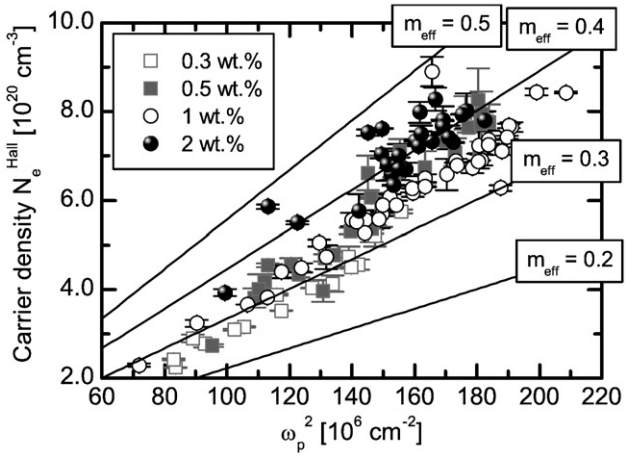

Fig. 2. Carrier density N_e^{Hall} as determined by Hall measurements as a function of the square of the plasma frequency obtained by modeling of optical spectra for sputtering targets with different aluminum content. The lines were calculated using Eq. (2) with the indicated values for the effective mass.

Despite the scattering a trend becomes clear: the data points do not follow a linear behavior as expected for a constant effective mass. While for low carrier concentrations the data points would be described by effective masses between 0.2 and 0.3 electron masses, an effective mass of $0.4 \cdot m_e$ would be required for higher carrier concentrations to explain the correlation. Thus the results suggest an increase of the effective mass with increasing carrier concentration.

In order to derive information on the form of the conduction band the linkage of the conduction band dispersion $E(k)$ and the effective mass m^*_{opt} has to be clarified. When transport properties are calculated, the so-called curvature or conduction effective mass should be considered. While the usual definition relating the effective mass to the inverse of the second derivative of the electron dispersion relates force to acceleration, the curvature effective mass is defined as the proportionality constant linking the electron velocity v_e to electron momentum $\hbar k$. Thus we obtain [23]

$$\frac{1}{m^*_{opt}} = \frac{v_e}{\hbar k} = \frac{1}{\hbar k}\frac{\partial \omega}{\partial k} = \frac{1}{\hbar^2 k}\frac{\partial E}{\partial k} \tag{7}$$

which is equivalent to the definition given in [24]. The expression has to be evaluated at the Fermi level. Eq. (7) will give the same result as the usual definition in the case of a parabolic band. In this case the curvature mass is also independent of the Fermi level.

The samples analyzed in this study are all highly degenerate, with the Fermi level being located well above the conduction band minimum and will be further shifted up with increasing doping. Thus, the trend shown in Fig. 2 is a clear indication for a non-parabolic conduction band. A simple from for a non-parabolic band is obtained when we add a quadratic term to the dispersion of the conduction band, yielding

$$\frac{\hbar^2 k^2}{2m^*_0} = E + C \cdot E^2, \tag{8}$$

where m^*_0 denotes the effective mass at the bottom of the conduction band and C is the non-parabolicity parameter.

For a dispersion as given by Eq. (8) Pisarkiewicz et al. [23] calculated the effective mass as a function of carrier concentration N_e. According to his result the effective mass can be written as

$$m^* = m^*_0\left(1 + 2C\frac{\hbar^2}{m^*_0}\left(3\pi^2 N_e\right)^{2/3}\right)^{1/2} \tag{9}$$

Fig. 3 shows the effective mass m^*_{opt} of various samples calculated from the plasma frequency ω_p and N_e^{Hall} by using Eq. (2) as a function of carrier concentration N_e. Unfortunately a fit of Eq. (9) to the whole dataset results in negative values for m^*_0 and agreement between theory and experiment is poor. Therefore, for further evaluation we decided to keep m^*_0 fixed. After studying literature extensively we concluded that $m^*_0 = 0.24 m_e$ is a reasonable value for m^*_0 [25].

With this fixed value of effective mass at the conduction band minimum we now fitted the data again, with the non-parabolicity parameter C being the only fitting parameter. It was found out that we obtain different values for C if we do the evaluation for data points grouped in respect to the aluminium concentration in the sputtering target. This does not mean that the samples of one group will all have the same aluminium concentration as a severe aluminium enrichment was observed for different deposition conditions [19].

Nevertheless, a good description was achieved for the samples deposited using the targets with an aluminum concentration of 0.5 or 1 wt.%. In these two cases the values obtained for C agree reasonably well, with C being equal to 0.251 eV^{-1} and 0.288 eV^{-1} for the target concentrations of 1 and 0.5 wt.%, respectively. In [26] Ellmer lists a value of 0.29 eV^{-1}, while Fujiwara et al., using the same approach as in our work, determine a value of 0.142 eV^{-1} for Ga-doped ZnO [9]. The discrepancy to the results of Fujiwara et al. is mainly caused by their assumption of $m^*_0 = 0.28 m_e$. An analysis of our data using different values for m^*_0 also leads to different values than the ones stated above. Thus the result should only be used to determine effective masses as a function of carrier concentration in the studied range. While we used an expression based on the approach by Pisarkiewicz in this work, other analytic expressions would in principle also describe the trend found in Fig. 3.

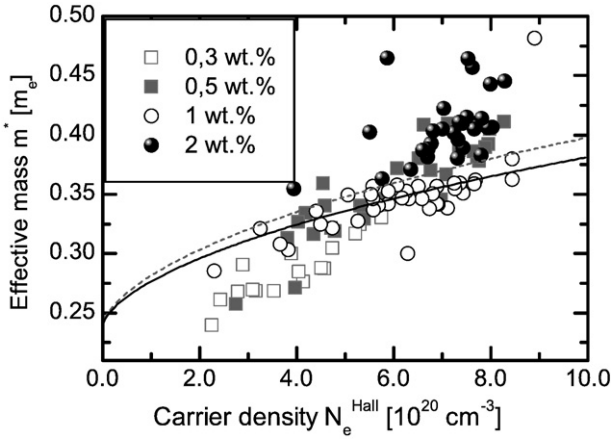

Fig. 3. Calculated effective mass m^*_{opt} as a function of carrier density N_e^{Hall} for samples deposited with different targets. The lines indicate fits of Eq. (9) to the data for the samples deposited using the target with an aluminum concentration of 0.5 (solid) and 1 wt.% (dashed).

For higher and lower target concentration the data points only spread over a smaller range of carrier concentrations, making an evaluation more difficult. Nevertheless, there is a trend to higher effective masses with higher target aluminum concentration of 2 wt.%, while the effective masses are below the fitted trends for lower target concentration of 0.3 wt.%. The reason for this is unclear and a correlation with aluminum concentration is difficult due to the aluminum enrichment already mentioned. It should just be stated that the average substrate temperature used during deposition was raised with decreasing target concentration, thus the films can grow with different morphologies. For instance the role of grain boundaries in our analysis is not clear, but there is evidence for decreased defect density at the grain boundaries at higher substrate temperatures [27].

It should be noted that Young et al. have determined higher effective masses using the method *of four coefficients* [28], so there will still be controversy over the form of the conduction band in highly doped ZnO thin films. Nevertheless, the values found by us can be used to calculate the carrier concentration in ZnO thin films from the optically determined plasma frequency, enabling a contact-free quality control in a production process.

4.3. Derivation of mobility from optical spectra

With the effective masses calculated as described in Section 4.2, Eq. (3) can now be used to determine the mobility μ_{opt} from the damping frequency. This has been done for the films deposited by using the targets with an aluminium concentration of 0.5 and 1 wt.% and the results, divided by mobility obtained from Hall measurements, are shown in Fig. 4.

For high carrier concentrations, namely above $5 \cdot 10^{20}$ cm^{-3}, most data points lie around unity. This means that the mobility derived from the modeling of optical spectra roughly matches the Hall mobility, although the error can be as high as 25%. This indicates that the free electrons seem to underlie the same scattering mechanism for movement under light excitation and in a DC field.

The situation changes when the carrier concentration is reduced. In this case the mobility determined with the damping frequency can be up to a factor of 3 higher than the mobility gained from Hall

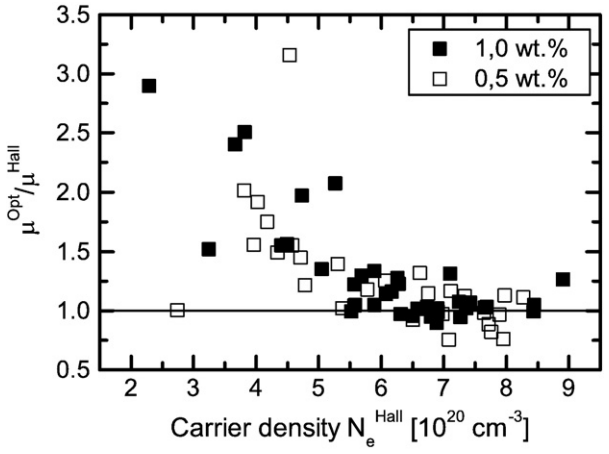

Fig. 4. Ratio of mobility determined from the damping frequency to the Hall mobility as a function of carrier concentration.

measurements. The main reason for this is grain boundary scattering, which gains an increasing importance in TCO films for lower carrier concentrations in the case of DC transport [29,30]. Apparently the electrons excited by light do not undergo grain boundary scattering. This can be explained by the low path length of the free electrons while moving in the high frequency electric field of the light.

The effect has been nicely demonstrated in the work of Steinhauser et al. [7], who compared optically determined mobilities with Hall mobilities for ZnO layers deposited by low pressure chemical vapor deposition (LPCVD). In their work the onset to increased grain boundary scattering is only at a much lower carrier concentration of around $1.5 \cdot 10^{20}$ cm^{-3}, which is caused by the larger grain size and lower defect density obtained for LPCVD layers.

The effect was also observed in μc-Si:H films where the microscopic electron mobility, determined by measurement of spin-relaxation times, was compared to macroscopic mobility determined by Hall measurements [31].

5. Summary

In summary we could show that recorded optical transmission and reflection data can be accurately modeled by using well known dispersion functions. While the Drude model can lead to small deviations the assumption of a frequency dependant damping term greatly increases the accuracy of the modeling. By using this model the plasma frequency can be accurately determined.

By combining the results from optical modeling with results obtained from Hall measurements it is possible to determine the curvature effective mass m^*_{opt} as a function of carrier concentration. It was found that the effective mass gained in this way depends not only on the carrier concentration alone but also slightly on the deposition conditions. If samples obtained from similar deposition conditions are considered, the data prove the non-parabolicity of the conduction band in ZnO and follow a simple form as given in Eq. (8). From our results we derived a non-parabolicity parameter C of ~0.27 ± 0.02 eV^{-1}, assuming a conduction band minimum effective mass m^*_0 of $0.24m_e$.

In principle also the mobility can be derived from the damping frequency obtained from optical modeling. If doing so it has to be considered that the optical damping parameters depends only on the intragrain scattering, while Hall mobility is also strongly influenced by grain boundary scattering for low carrier concentration. As shown by Ellmer [30] the carrier concentration, below which grain boundary scattering plays a significant role, depends on the defect density at the grain boundaries. This means that the deposition process and also the deposition conditions will play a significant role.

This distinct difference between Hall mobility μ^{Hall} and optical mobility μ^{opt} confirms that the determination of the resistivity ρ from optical data is only possible for high carrier concentrations. In this case it is also desirable to include optical data, that extends to energies well below the plasma frequency, e.g. infrared reflectivity spectra or infrared ellipsometry.

For lower doping concentrations the derivation of DC mobility from optical modeling seems to be impossible. Thus optical spectroscopy in this regime can mostly be used to monitor carrier concentration. This means optical spectroscopy will still have to be supported by electrical measurements in order to find the carrier concentration where the DC mobility is not limited by grain boundary scattering and thus maximized mobility is obtained.

Acknowledgements

The authors would like to thank W. Werner and A. Kaiser for their extensive work during sample preparation and C. Jacobs for carrying out optical measurements. We also like to thank our partners in the joint project LiMa. Funding of this project by the Federal Ministry for the Environment, Nature Conservation and Nuclear Safety BMU under contract No. 0327693H is gratefully acknowledged.

References

[1] D. Ginley, C. Bright (Eds.), MRS Bulletin, 25, 8, 2000.
[2] E. Fortunato, D. Ginley, H. Hosono, D.C. Paine, MRS Bulletin 32 (3) (2007) 242.
[3] For a recent review see. G.J. Exarhos, X.-D. Zhou, Thin Solid Films 515 (2007) 7025.
[4] We use the index *opt* in order to identify it as the quantity to be used in Eqs. 2 and 3. The calculation of m^*_{opt} is explained in Section 4.2. It should be noted that the tensor-character of the effective mass has to be considered for a non-spherical band. In the case of ZnO it seems reasonalbe to assume a spherical conduction band [5,28], thus our data analysis will not consider anisotropy.
[5] E.g. see. C. Klingshirn, Chem. Phys. Chem. 8 (2007) 782.
[6] S. Brehme, F. Fenske, W. Fuhs, E. Nebauer, M. Poschenrieder, B. Selle, I. Sieber, Thin Solid Films 342 (1999) 167.
[7] J. Steinhauser, S. Faÿ, N. Oliveira, E. Vallat-Sauvain, C. Ballif, Appl. Phys. Lett. 90 (2007) 142107.
[8] Z. Qiao, C. Agashe, D. Mergel, Thin Solid Films 496 (2006) 520.
[9] H. Fujiwara, M. Kondo, Phys. Rev. B 71 (2005) 075109.
[10] I. Volintiru, M. Creatore, M.C.M. van de Sanden, J. Appl. Phys. 103 (2008) 033704.
[11] E. Gerlach, J. Phys. C 19 (1986) 4585.
[12] I. Hamberg, C.G. Granqvist, Appl. Phys. Lett. 44 (8) (1984) 721.
[13] Z.-C. Jin, I. Hamberg, C.G. Granqvist, J. Appl. Phys. 64 (10) (1988) 5117.
[14] D. Mergel, Z. Qiao, J. Phys. D: Appl. Phys. 35 (2002) 794.
[15] A. Pflug, V. Sittinger, F. Ruske, B. Szyszka, G. Dittmar, Thin Solid Films 455–456 (2004) 201.
[16] Jin et al.[13] also proposed $\alpha = -2$ for ionized impurity scattering and found a good agreement in ZnO:Al.
[17] B. Szyszka, T. Höing, X. Jiang, A. Bierhals, N. Malkomes, M. Vergöhl, V. Sittinger, U. Bringmann, G. Bräuer, Society of Vacuum Coaters, 44th Annual Technical Conference Proceedings, Philadelphia, U.S.A., April 21–26 2001, p. 252.
[18] R.J. Hong, X. Jiang, V. Sittinger, B. Szyszka, T. Höing, G. Bräuer, G. Heide, G.H. Frischat, J. Vac. Sci. Technol. A 20 (3) (2002) 900.
[19] V. Sittinger, F. Ruske, W. Werner, B. Szyszka, B. Rech, J. Hüpkes, G. Schöpe, H. Stiebig, Thin Solid Films 496 (2006) 16.
[20] J. Leng, J. Opsal, H. Chu, M. Senko, D.E. Aspnes, Thin Solid Films 313–314 (1998) 132.
[21] D.A.G. Bruggeman, Annalen der Physik 416 (8) (1935) 665.
[22] ASTM/ANSI F76 – 73 (1973).
[23] T. Pisarkiewicz, A. Kolodziej, Phys. Stat. Sol. (B) 158 (1990) K5.
[24] N. Cavassilas, J.-L. Autran, F. Aniel, G. Fishman, J. Appl. Phys. 92 (3) (2002) 1431.
[25] S.J. Pearton, D.P. Norton, K. Ip, Y.W. Heo, T. Steiner, J. Vac. Sci. Technol. B 22 (3) (2004) 932.
[26] Table 2. K. Ellmer, J. Phys. D: Appl. Phys. 34 (2001) 3097.
[27] Unpublished data based on analysis of mobility versus carrier concentration and comparison to theories on grain boundary scattering.
[28] D.L. Young, T.J. Coutts, V.I. Kaydanov, A.S. Gilmore, W.P. Mulligan, J. Vac. Sci. Technol. A 18 (6) (2000) 2978.
[29] T. Minami, MRS Bulletin 25 (8) (2000) 38.
[30] K. Ellmer, R. Mientus, Thin Solid Films 516 (2008) 4620.
[31] K. Lips, P. Kanschat, W. Fuhs, Sol. Energy Mater. Sol. Cells 78 (2003) 513.